PREOPERATIVE EVALUATION OF VASCULAR MORPHOLOGY AND FUNCTION OF LIVING RENAL DONORS ON MULTI - DETECTOR ROW CT

Duong Phuoc Hung[1], Le Trong Khoan[2], Nguyen Khoa Hung[3]

DOI: 10.38103/jcmhch.2020.62.11

ABSTRACT:

Objectives: *Preoperative evaluation of the living renal donors vascular morphology and function with Multi-Detector CT (MDCT).*

Material and methods: *From Jan 2017 to August 2018, when carrying out a cross-sectional study at Cardiovascular Centre of Hue Central hospital, we have performed 64-MDCT with an unenhanced, three enhanced CT scan of arterial, parenchymal and secretory phase and two additional dynamic scans between the arterial and parenchymal phase to assess the renal vascular morphology and function on 154 living renal donors and proceeded to nephrectomy. Renal vascular morphology was compared with operational findings. Renal function calculated on MDCT by the Patlak equation was compared with single photon emission computed tomography (SPECT).*

Results: *154 living renal donors (male/female: 83.77%/16.23%), mean age was 30.72 ± 8.21 years (Range: 20-60 years). 154 chosen kidneys were proceeded to nephrectomy (right kidneys/left kidneys: 49.35%/50.65%), 76 right chosen kidneys (artery variation/vein variation: 20.51%/32.90%) and 78 left chosen kidneys (artery variation/vein variation: 10.53%/1.28%). CT findings all corresponded with the operation, and the sensitivity, positive predictive value, specialty, and negative predictive value of CT were all 100%. 100% of living donors have normal renal function in the excretory phase at 5 minute after CM and saline 0,9% injection bolus. This allows reducing examination time and radiation exposure with the highest effective dose 13.92mSv. The GFR from CT positively correlated with the GFR from SPECT. For the left kidney, the linear correlation coefficient was r = 0.822 (p < 0.001) and the linear regression model CT-GFR = 0.847 x SPECT - GFR + 8.513, (F = 317.410, p < 0.001, t = 3.090, p < 0.005). For the right kidney, the linear correlation coefficient was r = 0.824 (P < 0.001) and the linear regression model CT - GFR = 0.832 x SPECT - GFR + 9.433, (F = 320.424, p < 0.001, t = 3.831, p < 0.001).*

Conclusions: *MDCT contributes into not only more accurate diagnosis of the vascular morphology but also renal function calculation of living renal donors, helps surgeons make appropriate planning in the operation of chosen kidneys of living renal donors and transplanting into patients.*

Key words: *Renal vascular anatomy - Upper urinary tract - 64 MDCT - CT Urography - GFR*

1. Doctoral student, University of Medicine and Pharmacy, Hue University
2. University of Medicine and Pharmacy, Hue University
3. University of Medicine and Pharmacy, Hue University

Corresponding author: Duong Phuoc Hung
Email: duongphuochung@gmail.com
Received: 8/5/2020; **Revised:** 17/5/2020
Accepted: 20/6/2020

I. INTRODUCTION

Renal transplantation is currently the best available treatment option for patients of end-stage renal failure compared with other methods such as homeostasis and dialysis. Kidney evaluation of renal living donors for transplantation is one of the most important clinical features. Preoperative evaluation of anatomical characteristics of the vessels and renal function is one of the important purposes in living renal donors.

In recent years, with the continuous technical development of MDCT with thin slices, high resolution, good image quality and reconstruction of the vessels. MDCT with radiation exposure reduction, has been able to investigate the vascular morphology and evaluate renal functions.

From Jan 2017 to August 2018, Hue Central Hospital has deployed the technique of 64 - MDCT on the renal vascular and functional assessment to be applied on kidney transplantation. This has been contributing not only to the accurate diagnosis of the vascular morphology but also to the evaluation of single - kidney GFR, and providing useful information that helps surgeons plan their renal replacement surgery.

In this context, this research has been carried out to identify benefits of 64 - MDCT in the renal vascular and functional evaluation preoperative in living renal donors at Hue Central Hospital.

II. SUBJECTS AND METHODOLOGY

2.1. Subjects

154 cases of living renal donors were assigned to experience 64 - MDCT of the renal vessels and function from January 2017 to August 2018. Written informed consent was obtained from each patient.

2.2. Research facilities

Philips Brilliance 64 - MDCT and Medrad Stellant dual-injection machines.

2.3. Techniques

Conducting 64 MDCT technique of the renal vessels and function in living renal donors for:

- Assessment of the vascular morphology.
- Assessment of single - kidney GFR.

2.4. Patients preparation

- Abstaining from food 4 to 6 hours before scanning.
- Patients are given 750-1000 ml of water each 30 minutes before scanning and abstaining from urination for the purpose of secretory phase evaluation.

2.5. Multi-detector row CT protocol

An unenhanced and three enhanced CT scan of arterial, parenchymal, secretory phase and two additional dynamic scans to assess the kidney GFR between the arterial and parenchymal phase of the bilateral kidneys were performed using a 64 - MDCT in all the 154 patients. The patients were taught breath-holding.

2.6. Image technique

The following parameters were kept constant for each phase of scanning: section thickness of 2.0mm, reconstruction interval of 1mm, 0.5s rotation time, pitch factor of 1.171 and 120kVp; 80mAs (unenhanced phase scanning extent included the bilateral kidneys); 150mAs (arterial phase scanning extent included the common iliac vascular bifurcation for fear of the omission of the tiny accessory renal artery) using Bolus tracking technique with 30mAs, section thickness of 10mm, 1.5s rotation time and scanned at 10s after bolus injection (the region of interest: ROI of locator position inside the descending aorta at the level of the middle of bilateral kidneys hilum and the triggering threshold was set as 200 HU); 100mAs (parenchymal phase scanning extent included the bilateral kidneys) and (secretory phase scanning extent included the cavitas pelvis and was scanned at the only time of 5min after bolus injection of CM and saline 0,9%).

Two additional dynamic phases were scanned at the time about 50 - 55s and 65 - 70s between the

arterial and parenchymal phase with the following parameters: 120kVp, 30mAs, section thickness of 2.5mm, scanning time of 10s and pitch 1,171. Each dynamic phase included 5 scans, each scan took 2s at the middle of bilateral kidneys hilum.

Subsequently, an 18-gauge antecubital cannula was placed in an antecubital vein for bolus injection 1.0 - 1.5 mL/kg of ultravist or xenetix containing 300 mg of iodine per milliliter at a rate of 3 - 5 mL/s and then bolus injection 40ml of saline 0,9%.

2.7. Assessment of the glomerular filtration rate

Glomerular filtration rate (GFR) is the best index in clinical measurement of renal function. Inulin clearance is considered a gold standard for total GFR determination[16]. Contrast medium is similar in physiological nature to inulin[9]. Contrast medium clearance is an accurate method to assess glomerular filtration rate (GFR)[6]. The technique was first described by Rutland in 1979 for perfusion and background correction in renal scintigraphy. The Patlak-Rutland equation was developed by Patlak to measure the transfer constant of the blood–brain barrier [10]. This equation, the fundament of the CT - GFR calculation, is based on the two-compartment model with unilateral tracer flow from the first compartment (the vascular space) into the second compartment (the tubular space), while the intercellular space is negleted as a third compartment. The model is referred to as the whole kidney Patlak Equation when applied to the whole kidney. Since the increased density from tissues in enhanced CT is correspond to the concentration of contrast medium, equivalent to the proportion of the amount of iodine in the kidney, the increased value of the aorta and renal parenchyma can be used to estimate the amount of iodine in the kidney.

The whole kidney Patlak formula [6] can be expressed:

$$K(t) = B(t) + Q(t) \qquad (1)$$

The measured net attenuation of the whole kidney is named $K(t)$ measured in Hounsfield units (H), which is proportional to the amount of iodine in the kidney.

B (t) is proportional to the amount of contrast medium in the aorta [b (t)] and B (t) represents the net attenuation of the renal vascular space at time t after injection, indicating the amount of contrast medium in the renal vascular space.

$$B(t) = c1 \,.\, b \qquad (2)$$

where b (t) represents the net attenuation of the aortic lumen at time t after injection and c_1 represents a constant equivalent to the proportion of vascular space relative to the whole kidney volume.

Q (t) represents the net attenuation of the renal tubular compartment at time t after injection, indicating the amount of contrast medium in the renal tubular compartment. This value is proportional to the amount of contrast medium in the aorta.

$$Q(t) = c2\int_0^t b(t)\,dt \qquad (3)$$

where c_2 is equivalent to the clearance from the vascular space into the renal tubular compartment. Combining Equations. 1–3 leads to

$$K(t) = c1.b(t) + c2.\int_0^t b(t)\,dt \qquad (4)$$

When the integral of K(t) and b(t) (the scanning data of arterial and parenchymal phases, respectively) are known for two time points after injection (e.g., t_1 and t_2, which represent the scanning duration of arterial and parenchymal phases, respectively), the constant c_2 can be calculated from the resulting equation system:

$$K(t1) = c1.b(t1) + c2.\int_0^{t1} b(t)\,dt \qquad (5)$$

$$\text{and} \quad c2 = \frac{k(t2) - \dfrac{b(t2)}{b(t1)}.k(t1)}{\displaystyle\int_0^{t2} b(t)\,dt - \frac{b(t2)}{bt1)}.\int_0^{t1} b(t)\,dt} \qquad (6)$$

For calculation of GFR(CT), a correction for hematocrit has to be made because the density measurement of the iodine concentration in the aorta $b(t)$ (H/mm^3) belongs to full blood, whereas

the reference method measures plasma clearance. The hematocrit level of all patients was determined with a blood sample obtained just before CT.

GFR (CT) (mL/ min) was calculated according to equation 7:

$$GFR\ (CT) = (1 - Hct) \times c2 \quad (7)$$

2.8. Image processing and analysis

For the renal vascular morphology:

The CT data sets were transferred to a workstation for the anatomical manifestation of the main vessels and upper urinary tract by maximum intensity projection (MIP), multi-planar reconstruction (MPR), and volume rendering technique (VRT) procedures.

For the renal function:

At first, contour ROI (region of interest) of both kidney's parenchyma including cortex and medulla were segmented manually in the unenhanced scan, arterial and parenchymal phase for the mean CT number and slice area. The ROI was drawn as close as possible to the kidney surface. The structures in the renal hilum such as renal pelvis, vessels, and fatty tissue were excluded manually. It is possible to measure K (t) from CT images for a single kidney. Whole kidney attenuation of the left and right kidney (K) was calculated by multiplying mean density (H) by area (mm^2) and thickness (mm) for each kidney slice. K was calculated from the unenhanced scan, arterial and parenchymal phase. The net attenuation of the right and left kidney was calculated by subtracting the unenhanced kidney attenuation from kidney attenuation after contrast medium injection. $K(t)$ is the net attenuation of the kidney at time t.

Secondly, time density curve (TDC) was determined by the CT attenuation values of circular ROI in abdomen aorta. In our study, the aortic TDC was drawn from multiple time points at the level of the bilateral kidneys in the unenhanced scan, arterial phase, and parenchymal phase, and at the level of the renal hilum in the bolus triggering, dynamic phase I, dynamic phase II. Then, the whole attenuation of the abdominal aorta at each time point and its aortic TDC were calculated. The integral of the whole attenuation of the abdominal aorta [b (t)] for instances t_1 (arterial phase) and t_2 (parenchymal phase) was obtained.

Thirdly, All CT image data were transferred to a homemade software for further processing and calculating the single - kidney GFR.

2.9. SPECT examination

The Philips Brightview XCT single positron emission computed tomography (SPECT) system was used to detect renal hemodynamics and the dynamic collection of the urinary system for the single-kidney GFR. The SPECT examination was routinely carried out before or 48 h after the CT scan after venous injection of a glomerular filtration agent, ^{99m}Tc - DTPA (Diemethylenetriamine penta-acetic acid) 3 - 6 mCi (111 - 555MBq), via the ulnar vein by Bolus common syringes.

2.10. Methodology

Cross-sectional study, medical statistical analysis with SPSS version 20.0.

III. RESULTS

3.1. Living renal donors features

3.1.1. Age

Table 1: Donors (154) categorised by ages

Donor	Age		
	Youngest	Average ± SD	Oldest
	20	30.72 ± 7.21	60

The oldest living donor in our research was 60 years old

3.1.2. Gender

Table 2: Donors (154) categorized by genders

Donor	Gender			
	Male		Female	
	n	Percentage (%)	n	Percentage (%)
	129	83.77	25	16.23

The number of male living donors outnumbered that of female.

3.2. Vascular variation features in living renal donors

3.2.1. Anatomical variations of the artery preoperative

Table 3: Distribution of anatomical variations of the artery preoperative

The anatomical variations of the artery	**Right kidney**		**Left Kidney**	
	n	**Percentage (%)**	**n**	**Percentage (%)**
One artery	121	78.57	104	67.53
Two arteries (one main artery, one accessory artery)	26	16.88	45	29.22
Three arteries (one main artery, two accessory arteries)	7	4.55	4	2.60
Four arteries (one main artery, three accessory arteries)	0	0	1	0.65
Total	154	100	154	100

Kidneys had the majority of one artery, 78.57% at right kidneys and 67.53% at left kidneys.

Table 4: Distribution of anatomical variations of the early branching artery preoperative

The anatomical variations of the artery	**Right kidney**		**Left Kidney**	
	n	**Percentage (%)**	**n**	**Percentage (%)**
Normal branching artery	112	72.73	117	75.98
Early branching artery	42	27.27	37	24.02
Total	154	100	154	100

In our research, early branching artery was 27.27% at right kidneys and 24.02% at left kidneys.

3.2.2. *Anatomical variations of the vein preoperative*

Table 5: Distribution of anatomical variations of the vein preoperative

The anatomical variations of the vein	**Right kidney**		**Left Kidney**	
	n	**Percentage (%)**	**n**	**Percentage (%)**
One vein	102	66.23	151	98.05
Two veins (one main vein, one accessory vein)	47	30.52	3	1.95
Three veins (one main vein, two accessory veins)	5	3.25	0	0
Total	154	100	154	100

Kidneys had the majority of one vein, 66.23% at right kidneys and 98.05% at left kidneys.

Table 6: Distribution of anatomical variations of the late confluence vein preoperative

The anatomical variations of the vein	**Right kidney**		**Left Kidney**	
	n	**Percentage (%)**	**n**	**Percentage (%)**
Normal confluence vein	152	98.71	141	91.56
Late confluence vein	2	1.29	13	8.44
Total	154	100	154	100

In our research, late confluence vein was 1.29% at right kidneys and 8.44% at left kidneys.

3.2.3. Anatomical variations of the chosen kidneys artery preoperative and postoperative

Table 7: Distribution of anatomical variations of the artery preoperative and postoperative

The anatomical variations of the artery	**Right kidney**		**Left Kidney**	
	n	**Percentage (%)**	**n**	**Percentage (%)**
One artery	68	79.49	62	89.47
Two arteries (one main artery, one accessory artery)	7	19.23	15	9.21
Three arteries (one main artery, two accessory arteries)	1	1.28	1	1.32
Total	76	100	78	100

CT findings of anatomical variations of the artery preoperative all corresponded with the operation.

Table 8: Distribution of variations of the early branching artery preoperative and postoperative

The anatomical variations of the artery	**Right kidney**		**Left Kidney**	
	n	**Percentage (%)**	**n**	**Percentage (%)**
Normal branching artery	60	78.95	67	85.90
Early branching artery	16	21.05	11	14.10
Total	76	100	78	100

CT findings of anatomical variations of the early branching artery preoperative all corresponded with the operation.

3.2.4. *Anatomical variations of the chosen kidneys vein preoperative and postoperative*

Table 9: Distribution of anatomical variations of the vein preoperative and postoperative

The anatomical variations of the vein	**Right kidney**		**Left Kidney**	
	n	**Percentage (%)**	**n**	**Percentage (%)**
One vein	51	67.10	77	98.72
Two vein (one main vein, one accessory vein)	22	28.95	1	1.28
Three vein (one main vein, two accessory veins)	3	3.95	0	0
Total	76	100	78	100

CT findings of anatomical variations of the vein preoperative all corresponded with the operation.

Table 10: Distribution of variations of the late confluence vein preoperative and postoperative

The anatomical variations of the vein	**Right kidney**		**Left Kidney**	
	n	**Percentage (%)**	**n**	**Percentage (%)**
Normal confluence vein	75	98.69	75	96.15
Late confluence vein	1	1.31	3	3.85
Total	76	100	78	100

CT findings of anatomical variations of the late confluence vein preoperative all corresponded with the operation.

3.3. The renal function evaluation on 64 - MDCT

3.3.1. The renal secretory function evaluation on 64-MDCT

Table 11: Distribution of visualization time of CM in the upper urinary tract

Visualization time of CM in upper urinary tract	Right kidney		Left kidney	
	n	Percentage (%)	n	Percentage (%)
5 min after bolus injection of CM and saline	154	100	154	100
Total	154	100	154	100

We finded CM excreted into the upper urinary tract in both kidneys when the secretory phase was scanned at the only time of 5 minute after bolus injection of CM and saline 0,9% in all of cases.

3.3.2. The glomerular filtration rate evaluation

Table 12: Distribution of GFR from CT and GFR from SPECT

GFR		n	Minimum	Maximum	Mean	SD	p value
Left kidney	CT-GFR	154	42.30	80.21	57.2173	7.34605	p = 0,699 p > 0,05
	SPECT-GFR	154	41.80	76.80	57.5366	7.13610	
Right kidney	CT-GFR	154	40.02	72.91	53.1715	6.56888	p = 0,414 p > 0,05
	SPECT-GFR	154	40.10	71.00	52.5651	6.45905	

There is no statistically significant difference between the calculation of GFR from CT and GFR from SPECT for the left and the right kidney.

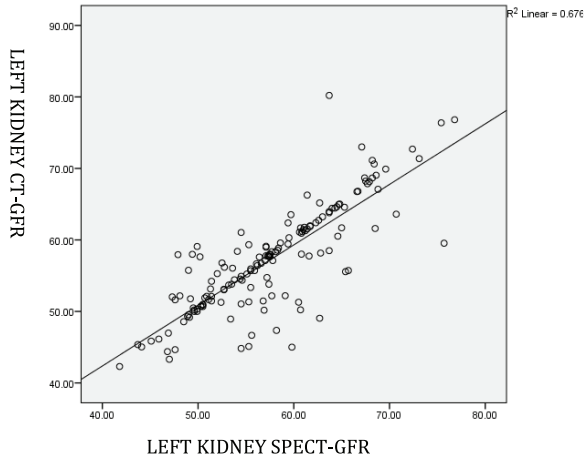

Figure 1: Regression of the GFR from CT and GFR from SPECT for the left kidney

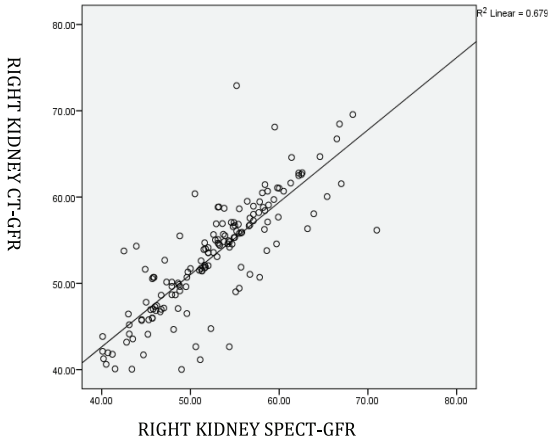

Figure 2: Regression of the GFR from CT and GFR from SPECT for the right kidney

	Left kidney
R	+ 0.822
R^2	0.676
P	< 0.001
y =	0.847x + 8.513
	y: CT-GFR, x : SPECT-GFR

	Right kidney
R	+ 0.824
R^2	0.679
P	< 0.001
y =	0.838x + 9.123
	y: CT-GFR, x : SPECT-GFR

3.4. Evaluation of radiation exposure on 64-MDCT with six phases scanning

Table 13: Distribution of radiation exposure on 64-MDCT with six phases scanning

Effective dose (mSv)		
Lowest	**Average**	**Highest**
12.99mVs	13.40mSv	13.92mSv

The highest effective dose was 13.92mSv in our study

3.5. Imaging illustrations of the vascular features in living renal donors

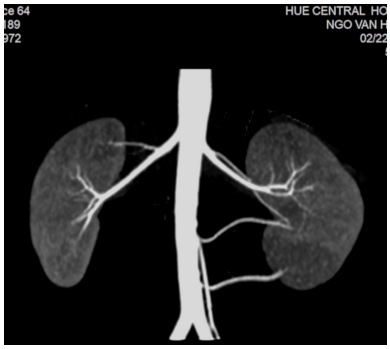

Figure 3: Three arteries in left kidney, early branching artery in right and left kidney

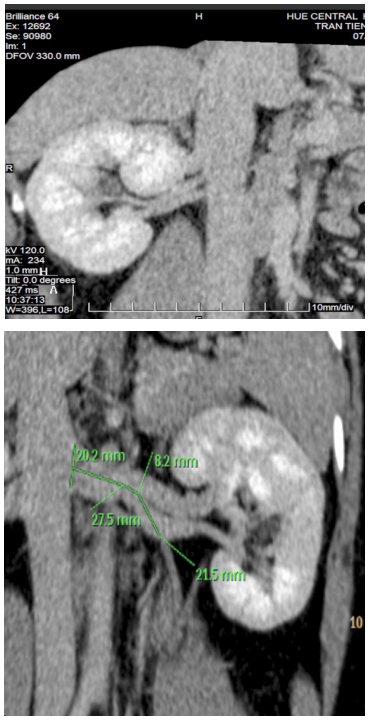

Figure 4: Three veins in right kidney, late confluence vein in left kidney

IV. DISCUSSION

Evaluating the anatomical characteristics of the vessels and upper urinary tract in living renal donors prior to selection of kidney for transplantation bares critical purposes. It helps surgeons plan their renal removal surgery for renal transplantation.

In our research, CT findings of anatomical variations of the main artery, accessory artery, early branching artery; main vein, accessory vein and late confluence vein of all chosen kidneys prepoperative all corresponded with the operation, and the sensitivity, positive predictive value, specialty, and negative predictive value of CT were all 100%. This result corresponds well with those of Su et al. (2010) [12], Baratali (2013) [1] and Steven et al. (2006) [11].

64-MDCT can assess well the information of renal function. We scanned the secretory phase at the only time of 5min after bolus injection of contrast media (CM) and saline 0,9% and found that all cases of CM excretion to the upper urinary tract were oberved in both kidneys. This allows us to conclude that all living donor cases in our study had well-functioning two kidneys and that results in a reduction of the examination time. Claebots C. et al. has used MDCT technique to examine urinary tract combined with hyperdiuresis method by intravenous furosemide injection ($\leq$ 0 mg) immediately prior to CM injection, which helps reduce from 5 to 7.5 minutes of the examination time [2].

The purpose of preoperative assessment in living renal donors is to determine whether the donor retains a normal kidney that functions well after the other kidney is removed.

In our study, we performed the CT scanning protocol to allow not only assessing the preoperative vascular anatomy but also function of living renal donors without acute renal disorder by calculating the CT - GFR using the Patlak Equation.

It is important to assess renal function in living renal donors to avoid renal failure during the remainder of their life. Therefore, Preoperative evaluation of donor single - kidney GFR is

extremely important to decide the laterality of donor nephrectomy.

Several studies have compared CT with nuclear renography to estimate single - kidney GFR and showed a strong correlation between the two techniques in preoperative living kidney donors and in patients with clinical diseases.

In 1986, O'Reilly et al. [9] concluded that the plasma clearance of non-ionic iodine contrast medium can be used to asessss the single-kidney GFR via spiral CT and this procedure played a useful role in standard clinical practice.

In 1993, Dawson and Peters [3] first described a study employing the bolus contrast dynamic CT (5 s/scan for 2 min in a fixed single slice) after the injection of 40 mL of contrast medium to measure the single-kidney GFR using Patlak equation with a high degree of statistical confidence.

In 1999, Tsushima et al. [13] calculated the CT - GFR using single-location, dynamic CT and a fixed 10-mm thick slice was repeatedly scanned for 18 times with a bolus injection of 40 mL of contrast material during 85s and found a strong correlation between the CT - GFR and 24 h creatinine clearance rate of 0.87; and for 13 times with a bolus injection of 20 mL of contrast material during 96s and found a stronger correlation between the CT - GFR and 24 h creatinine clearance rate of 0.92 in 2001 [14] after correction for Hct.

In 2002, Hackstein et al. [4] calculated the CT - GFR using the CT protocol consisted of an unenhanced scan and three subsequent contrast-enhanced scans 45, 75, and 105s and found a best correlation between the CT - GFR and plasma clearance rate of 0.84 in 50 adult patients without acute renal disorder and Hct for all patients at 0.36; and 38, 71, and 102s and found a significant correlation between the CT - GFR and plasma clearance rate of 0.80 in 20 adult patients treated with percutaneous nephrostomy in 2003 [5] after starting an injection of 120 mL of iopromide using an injection rate of 3 mL/s.

In 2004, Hackstein et al. [6] used 4 - slice spiral CT and added 12 dynamic scans between the arterial phase and venous phase and obtained a corresponding CT value for the aorta. These authors found that the correlation coefficients between the CT - GFR and the GFR from iopromide plasma clearance was 0.889 with GFR (CT) = 15 + 0.83 × GFR (iopromide plasma clearance) in 50 patients without acute renal disorder after correction for Hct.

In 2010, Su et al. [12] employed 64-slice spiral CT and inserted two dynamic scans between the cortical and parenchymal phases in the regular scans to get more accurate information for the time-density curve of the aorta as well as more accurate determination of the GFR in 21 living renal donors and indicated the GFR from CT positively correlated with the GFR from DTPA/SPECT. For the left kidney, the linear correlation coefficient was $r = 0.894$ ($p < 0.001$) and the linear regression model GFR (CT) = 1.917 + 0.883 x GFR (SPECT). For the right kidney, the linear correlation coefficient was $r = 0.881$ ($p < 0.001$) and the linear regression model GFR (CT) = 7.713 + 0.753 x GFR (SPECT).

In 2014, Helck et al. [7] calculated the CT-GFR by a modified Patlak method and compared with the split renal function obtained with renal scintigraphy in 7 healthy potential kidney donors using a 128-slice CT - scanner with continuous bi-directional table movement, allowing the coverage of a scan range of 18 cm within 1.75 sec. Twelve scans of the kidneys ($n = 14$) were acquired every 3.5 seconds. These authors found that GFR obtained from dynamic CTA correlated well with renal scintigraphy with a correlation coefficient of $r = 0.84$; $p = 0.0002$.

In 2015, Kwon et al. [8] used 64 - section CT to calculate the CT-GFR after correction for Hct in 96 hypertensive patients after correction for Hct and found that among all kidneys, means ± standard deviations of single-kidney CT GFR (38.2 mL/min ± 18.6) and iothalamate GFR (41.6 mL/min ±

17.3) were not significantly different (p = 0.062). CT GFR correlated well with iothalamate GFR with a concordance coefficient correlation r = 0.835 and the linear regression CT GFR = 0.88*iothalamate GFR, r^2 = 0.89, p < 0.0001.

In 2016, Zhang et al. [17] employed the 128-slice CT scanner performing the triphasic CT examination (non-enhanced scan, arterial scan triggered by the bolus tracking technique inside the aorta at the level of the supraceliac abdominal aorta, and parenchymal scan) for calculating Split Kidney GFR (SKGFR) between CT and ^{99m}Tc-DTPA/SPECT by using Modified Two Points Patlak (MPT-Patlak) in 13 patients after correction for Hct of 0.42 for all subjects. The authors showed that the linear correlation between the two methods was r = 0.75 (p < 0.01). The mean difference between SKGFRs as determined with the two methods was 7.4 ± 9.0 mL/min. Hct of 0.42 for all subjects. The MTP-Patlak approach, featured with simplicity, is feasible in a clinically indicated CT examination for the evaluation of split renal function.

In 2019, Wang et al. [16] used the first-generation dual-source CT scanner performing the modified multiphasic CT scans of the whole kidneys for calculating CT-GFR using Patlak plot in 91 patients with unilateral renal tumor (all patients had no acute renal disorders) consisted of a plain scan, an arterial phase (triggered by the bolus tracking technique inside the aorta at the level of renal hilum), an early parenchymal phase and a late parenchymal phase, respectively, and an additional dynamic scan (15 scans at the level of renal hilum) between arterial phase and early parenchymal phase after correction for Hct. They found a strong correlation between CT-GFR with renal tumor and estimated GFR with the linear regression y = 19.82 + 0.86x (r = 0.90, p < 0.001) in early renal parenchymal phase and the relative CT - GFR in early renal parenchymal phase was highly correlated with the relative Radionuclide-GFR with the linear regression y = 25.14 + 1.5x (r = 0.88, p < 0.001). The Hct among all the study population was 0.40 ± 0.04.

In our study, after correction for Hct (0.38 ± 0.03). the GFR from CT positively correlated with the GFR from SPECT. This result corresponds well with those of the above authors.

64 - MDCT protocol in our study has been found to meet the requirement for reducing radiation doses at living donors, while also meeting the diagnostic criteria for determining renal vascular characteristics and function in limiting the scanning field, decrease kV, change mAs accordingly [13]. The highest effective dose in our study using 64-MDCT with six phases was 13.92 mSv, which was lower with three-phase scanning of the entire abdomen radiating with an effective dose of 15 - 25 mSv by Van Der Molen AJ. and al. [13]. It is important to note that the ideal technical procedures is to produce good quality images, but with limited radiation doses, according to the ALARA principle.

V. CONCLUSION

Through a study on 64 - MDCT of the renal vascular morphology and function on 154 living donors, we have found that MDCT offers satisfactory results in evaluating renal vessel anatomy and variations and has been recognized by transplantation surgeons.

64 - MDCT evaluates accurately not only the vascular anatomy, but also the renal function of living donors. It helps reduce examination time and radiation dose in all cases, which helps surgeons plan for a renal operation from selected kidney of the living donors and implementation of kidney transplants for patients.

REFERENCES

1. Baratali A. (2013), "Role of Multidetector Computed Tomography for Evaluation of Living Kidney Donors", Published online 2013 Aug 12. doi: 10.5812/numonthly. 10875.

2. Claebots C., Puech P., Delomez J., Devos P.L. (2007), "MDCT urography with and without use of diuretics", *J Radiol* 2007; 88: 1697 - 702.
3. Dawson P., Peters M. (1993), "Dynamic contrast bolus computed tomography for the assessment of renal function", *Invest Radiol*, 28: 1039 - 1042.
4. Hackstein, N., Cengiz, H., and Rau, W. S. (2002), "Contrast media clearance in a single kidney measured on multiphasic helical CT: results in 50 patients without acute renal disorder", *AJR Am. J. Roentgenol,* 178, 111 - 118. doi: 10.2214/ajr. 178. 1.1780111.
5. Hackstein, N., Bauer, J., Hauck, E. W., Ludwig, M., Kramer, H. J., and Rau, W. S. (2003), "Measuring single-kidney glomerular filtration rate on single-detector helical CT using a two-point patlak plot technique in patients with increased interstitial space", *AJR Am. J. Roentgenol,* 181, 147 - 156. doi: 10.2214/ajr.181.1. 1810147.
6. Hackstein N., Wiegand C., Rau W.S., Langheinrich A.C. (2004), "Glomerular filtration rate measured by using triphasic helical CT with a two-point Patlak plot technique", *Radiology*, 230: 221 - 226.
7. Helck A., Scho - nermarck U., Habicht A., Notohamiprodjo M., Stangl M., et al. (2014), "Determination of Split Renal Function Using Dynamic CT-Angiography: Preliminary Results", *PLoS ONE 9(3),* e91774. doi: 10.1371/journal. pone. 0091774.
8. Kwon, S. H., Saad, A., Herrmann, S. M., Textor, S. C., and Lerman, L. O. (2015), "Determination of single-kidney glomerular filtration rate in human subjects by using CT", *Radiology,* 276, 490–498. doi: 10.1148/radiol.2015141892.
9. O'Reilly P.H., Brooman P.J., Martin P.J., et al. (1986), "Accuracy and reproducibility of a new contrast clearance method for the determination of glomerular filtration rate", *Br Med J (Clin Res Ed),* 293: 234 -236.
10. Patlak C.S., Blasberg R.G., Fenstermacher J.D. (1983), "Graphical evaluation of blood - to - brain transfer constants from multiple - time uptake data", *J Cereb Blood Flow Metab,* 3: 1 - 7.
11. Steven S.R. et al. (2006), "Utility of 16 - MDCT Angiography for Comprehensive Preoperative Vascular Evaluation of Laparoscopy Renal Donors", *AJR*, volume 186, Number 6.
12. Su C. et al. (2010), "Multi-detector row CT as a ''one-stop'' examination in the preliminary study", *Abdom Imaging* (2011) 36: 86 - 90.
13. Tsushima Y., Blomley M.J., Kusano S., Endo K. (1999), "Use of con - trast - enhanced computed tomography to measure clearance per unit renal volume: a novel measurement of renal function and fractional vascular volume", *Am J Kidney Dis*, 33: 754 - 760.
14. Tsushima Y., Blomley M.J., Okabe K., Tsuchiya K., Aoki J., Endo K. (2001), "Determination of glomerular filtration rate per unit renal volume using computerized tomography: correlation with conventional measures of total and divided renal function", *J Urol*, 165: 382 - 385.
15. Van Der Molen A.J., Cowan N.C., Mueller-Lisse U.G., Nolte-Ernsting C.C., Takahashi S., Cohan R.H. (2008), "CT urography: definition, indications and techniques. A guideline for clinical practice", *Eur Radiol,* 18(1), pp. 4 - 17.
16. Wang T., Xu Y., Liu W., Shao P., Lv Q., Yang G. and Tang L. (2019), "Measurement of Glomerular Filtration Rate Using Multiphasic Computed Tomography in Patients With Unilateral Renal Tumors: A Feasibility Study", *Front. Physiol,* 10: 1209. doi: 10.3389/fphys.2019. 01209.
17. Zhang Y.D., Xue C.Q., Wu C.J., Tao J., Zhou W.L., Shi H.B. (2016), "Feasibility of triphasic CT with a modified two-point Patlak plot to determine spit kidney glomerular filtration rate in clinical practice", *Abdom Radiol*, DOI: 10.1007/s 00261 - 016 - 0858 - 9.